The Interdiffusion of Polymers

Jacob Klein

Science, New Series, Volume 250, Issue 4981 (Nov. 2, 1990), 640-646.

---

4. G. C. Myers and K. Manton, in *Aging: The Universal Human Experience*, G. L. Maddox and E. W. Busse, Eds. (Springer, New York, 1987), pp. 263–283.
5. R. G. Rogers and R. Hackenberg, *Soc. Bio.* **34**, 234 (1988).
6. S. R. Johansson, *Aging and Dying: The Biological Foundations of Human Longevity* (Univ. of California Press, Berkeley, in press).
7. E. Crimmins, Y. Saito, D. Ingegneri, *Pop. Dev Rev* **15**, 235 (1989).
8. J. F. Fries, *Perspec. Biol. Med.* **31**, 407 (1988).
9. S. Katz *et al.*, *N. Engl. J. Med.* **309**, 1218 (1983).
10. R. G. Rogers, A. Rogers, A. Belanger, *Milbank Q.* **67**, 370 (1989).
11. E. L. Schneider and J. M. Guralnik, *Gerontol. Perspec.* **1**, 8 (1987).
12. B. J. Soldo and K. G. Manton, *Milbank Mem. Fund Q* **63**, 286 (1985).
13. H. S. Shryock and J. S. Siegel, *The Methods and Materials of Demography* (Bureau of the Census, Washington, DC, ed. 3, 1975), vol. 2, p. 433.
14. J. F. Fries, *Milbank Q.* **67**, 208 (1990).
15. J. Bourgeois-Pichat, *Pop. Bull. U.N.* **11**, 12 (1978).
16. K. G. Manton, M. A. Woodbury, E. Stallard, in *Aging and Dying: The Biological Foundations of Human Longevity*, S. R. Johansson, Ed. (Univ. of California Press, Berkeley, in press).
17. J. S. Siegel, *NIH Publ. 80-969* (1980), pp. 17–82.
18. N. B. Ryder, [*Pop Index* **41**, 3 (1975)] has developed a variant of this method using model life tables.
19. R. G. Cutler, *Gerontol. Biomed. Acta* **1**, 35 (1986).
20. R. Havighurst and G. A. Sacher, in *Extending the Human Life Span: Social Policy and Social Ethics*, B. Neugarten and R. Havighurst, Eds. (Univ. of Chicago Press, Chicago, 1977), pp. 13–18.
21. N. G. Bennett and L. K. Garson, *Gerontologist* **26**, 358 (1986).
22. ——, *Demography* **20**, 587 (1983).
23. R. B. Mazess and S. H. Forman, *J. Gerontol.* **34**, 94 (1979).
24. Z. A. Medvedev, *Gerontologist* **14**, 381 (1974).
25. A. H. Wade, "United States life table functions and actuarial functions based on the alternative II mortality probabilities used (Social Security Administration, Office of the Actuary, Washington, DC, 1988).
26. C. L. Chiang, *Introduction to Stochastic Processes in Biostatistics* (Wiley, New York, 1968).
27. F. R. Bayo and J. C. Wilkin, Actuarial Study 74, *HEW Publ.* (SSA) 77-11521 (1977).
28. A. H. Wade, Actuarial Study 104, Social Security Administration, Office of the Actuary, *HEW Publ.* (SSA) 11-11551 (1989).
29. N. W. Shock, in *The Biology of Aging*, B. L. Strehler, J. D. Ebert, H. B. Glass, N. W. Shock, Eds. (American Institute of Biological Sciences, Washington, DC 1960), pp. 14–29.
30. K. G. Manton, *J. Gerontol.* **41**, 672 (1986).
31. S. H. Preston, N. Keyfitz, R. Schoen, *Causes of Death: Life Tables for National Populations* (Seminar Press, New York, 1972).
32. National Center for Health Statistics, *Vital Statistics of the United States: 1985.* (DHHS Publ. No. (PHS) 88-1101, U.S. Department of Health and Human Services, Washington, DC, 1988), vol. 2, part A.
33. J. F. Fries, *N. Engl J Med.* **303**, 130 (1980).
34. J. M. Alho, *Demography* **26**, 705 (1989).
35. N. Keyfitz, *Applied Mathematical Demography* (Springer, New York, ed. 2, 1985).
36. J. H. Pollard, *Demography* **25**, 265 (1988).
37. G. C. Myers and K. Manton, *Gerontologist* **24**, 346 (1984).
38. R. Rothenberg, H. R. Lentzner, R. A. Parker, *J. Gerontol*, in press.
39. S. J. Olshansky, *ibid.* **42**, 358 (1987).
40. ——, *Milbank Q.* **66**, 482 (1988).
41. J. M. Guralnik, M. Yanagashita, E. L. Schneider, *ibid.*, p. 283.
42. L. M. Verbrugge, *Annu. Rev. Publ. Health* **10**, 333 (1989).
43. J. A. Brody, *Nature* **315**, 463 (1985).
44. J. A. Brody, in *Ethical Dimensions of Geriatric Care, Value Conflicts for the 21st Century*, S. F. Spicker, S. R. Inhman, I. R. Lawson, Eds. (Rieidel, Dordrecht, Holland, 1984), pp. 3–22.
45. E. L. Schneider and J. M. Guralnik, *J. Am. Med. Assoc.* **263**, 2335 (1990).
46. L. M. Verbrugge, *Milbank Mem. Fund Q.* **62**, 475 (1984).
47. E. M. Greunberg, *ibid.* **55**, 3 (1977).
48. M. Kramer, *Acta Psychiatr. Scand Suppl.* **285**, 382 (1980).
49. The authors wish to thank P. Meier, B. Neugarten, J. Alho, J. F. Fries, R. Rogers, and anonymous reviewers for comments on an earlier draft of this manuscript; L. S. Haley and M. J. Koelbl for preparation of the figures, and a special thanks to John Hoffecker. Supported by a grant from the National Institute on Aging AG06996-01.

The Interdiffusion of Polymers

JACOB KLEIN

In contrast to interdiffusion in simple liquids, interdiffusion of polymeric chains is dominated by their intertanglement and their large size. These properties profoundly reduce both the molecular mobilities and the role of entropy in driving the mixing. The resulting diffusional processes have only recently been studied. Such studies reveal a wide spectrum of behavior ranging from accelerated interdiffusion (for strongly compatible chains) to its suppression below the critical point for phase separation. Effects that are still poorly understood include the initial disposition at interfaces of the chains' ends (through which diffusion proceeds by reptation) and the need for cooperative motion, which can strongly magnify local friction.

Mixing of liquids is commonplace. At the molecular level, it takes place by diffusion: to what extent and how rapidly liquids interdiffuse depend on their chemical affinity and on the mobility of their molecules. For simple liquids (composed of small molecules), mixing is classical and well understood (*1, 2*). In the case of polymers, on the other hand (both synthetic chains and flexible biopolymers), the large size of the molecules together with their intertangled nature result in extremes of sluggishness and molecular incompatibility (or, in rare cases, extreme compatibility). For these reasons, it is only recently that insight into the process of mixing different polymers, based on direct measurements of their interdiffusion, is emerging.

The connected, chain-like nature of polymer molecules leads to entanglements. These arise because the backbones of the polymer chains cannot cross through each other (Fig. 1); motion involving such mutual crossing is forbidden. This effect is most marked in undiluted polymeric liquids (*3*), where every chain is highly interpenetrated by others. In such a polymer melt (N monomers per chain), each chain adopts on average an open, random, coil-like conformation (*4, 5*). For typical values of N in the range 10^3 to 10^4, only about 1% of the volume of such a coil is occupied by the monomers of the chain itself: the rest of the coil volume is interpenetrated and filled by segments belonging to other chains.

The author is in the Department of Polymer Research, Weizmann Institute of Science, Rehovot 76100, Israel.

The work of Edwards, starting in the 1960s (*6*), first indicated how entanglements may be dealt with in terms of topological constraints on the motion of molecules: the mutual noncrossability of chain contours, the essential constraint, is accounted for by limiting the lateral motion of any chain (normal to its contour) so that chains are confined effectively within a "tube" or "pipe." In 1971, de Gennes considered the diffusion of a single flexible chain moving by Brownian motion in a network of fixed obstacles (*7*); he suggested that the chain would move by random curvilinear motion, essentially along its own contour within a "tube" defined by the obstacles, and thereby avoid the large sideways motion that necessitates crossing through obstacles. This type of motion was termed reptation, to describe the random creeping or slithering of the chain. A basic law for diffusion by reptation relates the translational diffusion coefficient D_L of entangled linear chains to their degree of polymerization N,

$$D_L = D_1/N^2 \qquad (1)$$

where D_1 is a diffusion coefficient typical of the Brownian motion of a single monomer. Although D_1 depends on the detailed chemistry of the particular polymer through local friction coefficients, the inverse square law (Eq. 1) is a direct consequence of constraining a flexible, random-walk chain to curvilinear Brownian diffusion (reptation) and is expected to be universal for entangled chains. Since the first experimental demonstration of Eq. 1 in 1978 (*8*), the reptation concept has been confirmed by many studies (*9*) and has become the basis for understanding the diffusive motion of entangled chains at the molecular level (*10*). This is true not only in fixed networks [for example, DNA chains in a gel column (*11*)] but also in a polymeric liquid consisting of many mobile chains (as long as N exceeds about 200), where the "tube" about any given chain is defined by the constraints on it due to its neighbors (*8–10, 12*) (Fig. 1).

In addition to the topological constraints on the self- or tracer-diffusion of entangled chains, polymer-polymer interdiffusion differs from interdiffusion in small-molecule liquids for thermodynamic reasons (*4, 5*). With notable exceptions, interactions in polymeric liquids or melts are dominated by dispersive (van der Waals) interactions, where like prefers like, and the mixing of different monomers is energetically unfavorable (*4, 5, 13*). A measure of this is given by $\chi k_B T$, the interaction energy cost of surrounding one type of monomer by another type of monomer, where the value of χ [known as the Flory-Huggins parameter from the classical theory of polymer mixing due to these workers (*4*)] is a measure of their chemical compatibility, k_B is the Boltzmann constant, and T is the temperature.

As in the binary solution theory of simple liquids (*1*), the net interaction energy change for creating a polymer mixture with local volume fractions ϕ and $(1 - \phi)$ of the two species is proportional to $\chi\phi(1 - \phi)$. This energy change is generally positive and opposes mixing. But there is a crucial difference in the factors that drive the interdiffusion: the increase of combinatorial entropy on mixing polymeric molecules is reduced, relative to that of mixing small molecules, by the number of monomers N on each chain. This is because the number of independent (polymeric) molecules in a given volume is also smaller by that factor. As N is very large, the gain in mixing entropy is correspondingly small, and the overall mixing is dominated by the monomeric interactions. This is why different polymers are, in general, only slightly miscible with each other (*4, 5, 13*): mixing is promoted by an entropy gain that is proportional to the number of polymer chains but must take account of (usually unfavorable) interactions proportional to the much larger number of contacts between monomers. The nature of the monomeric interactions, expressed in χ, not only may affect the final extent of mixing but also may dominate the rate at which two different polymers interdiffuse.

Interdiffusion of polymers is implicated in a wide range of phenomena [see reviews in (*9*)]. These include adhesion and bonding between polymeric materials, the flow and viscoelastic properties of polymer blends and mixtures, and, in a more general sense, effects that are associated with the dynamics of chains in confined geometries, as in thin films, micropores and microspheres, and at surfaces. The process of self-organization of polymeric amphiphiles and the development of microstructure in block copolymers and in polymeric alloys are also intimately related to their mutual diffusion. Insight into the factors that underlie these phenomena is best obtained from direct studies of the interdiffusion process.

Measuring Polymer Interdiffusion

Diffusion coefficients that control the mixing of small molecules in liquids have values around 10^{-5} cm^2 s^{-1} (*2*), but the earliest measurements showed that diffusion rates in molten polymers could be several orders of magnitude smaller (*14*). The emergence in the 1970s of the molecular theories of diffusion (*7, 15*), based on the reptation concept of entangled chains, proved a challenge to experimentalists to measure self-diffusion, and, more recently, mutual (or inter-) diffusion between different polymers, on increasingly finer scales.

Interdiffusion of polymers controls a host of physical properties (*9*), but experiments that yield concentration profiles across an interface between the two polymeric species provide the most direct measure. The detailed shape of such profiles, as well as their width, and the way these vary with time, contain in principle all the information on the interdiffusion process (*16*); in particular, they reflect the variation of the mutual diffusion rate with local composition and can be used to derive the molecular mechanisms that

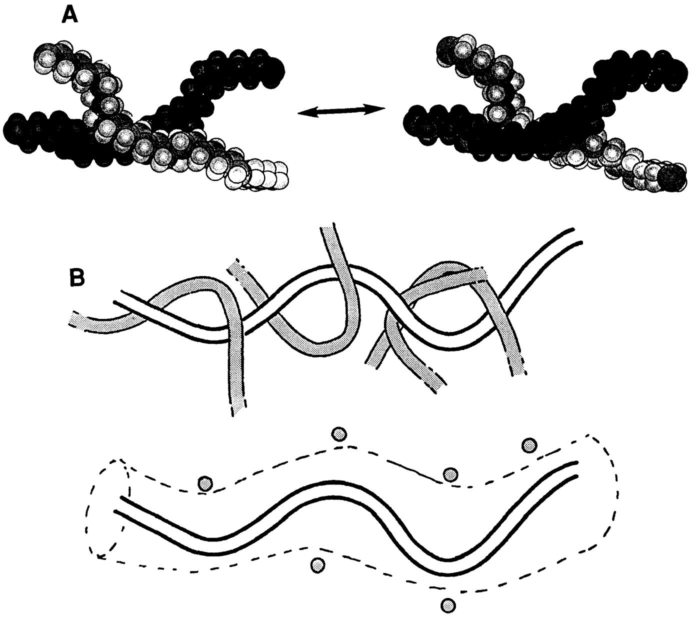

Fig. 1. (**A**) Illustration of the entanglement effect: the transition shown, which involves chain contours crossing laterally through each other, is forbidden (for clarity, only a short segment of each chain is shown). (**B**) Entanglements of a chain with its neighbors (shaded, top) in a melt result in a constraining "tube" about the chain defined by the locus of its intersections with the other chains (bottom, schematically showing sections of the constraining chains in a plane parallel to the paper).

control it. A common approach is to create a sharp interface between the polymers and observe at a later time how it has broadened as a result of interdiffusion, using for the purpose some signal that differentiates the two components. The most convenient (and chemically nonperturbing) labels are provided by isotopic substitution or sometimes the presence of heavy atoms on one of the polymers or marker atoms at the interface. Techniques include infrared microdensitometry (*17*), microanalytical electron microscopy (*18, 19*), etching methods combined with mass spectrometry (*20*), neutron (*21*) and x-ray (*22*) reflection methods, and ion-beam scattering (*23*). These methods have been used to investigate interdiffusion associated with diffusion rates D covering the range from 10^{-6} to 10^{-18} cm^2 s^{-1}. At the lower end of the range, such D values correspond to a motion of the molecules of only some 100 Å a day (*24*), so that spatial resolution is clearly at a premium.

Of the methods that yield concentration profiles directly, ion-beam scattering methods (Rutherford backscattering and elastic recoil spectroscopy), extended to the study of polymer interdiffusion by Kramer and Mayer and their co-workers at Cornell (*23, 25*), considerably improved the spatial resolution of earlier techniques and have been widely applied. These techniques provide a measure of interdiffusion on a scale from a few hundred to several thousand angstroms, mainly through the use of isotopic labeling (*25*), where protons are replaced by deuterium atoms on the chains. A technique very recently developed in our laboratory, based on nuclear reaction analysis, provides an even higher spatial resolution (around 100 Å). It has been used to determine interdiffusion profiles between two polymers, of which one is deuterated (*26*). The experimental configuration (Fig. 2) relies on the nuclear reaction $^3\text{He} + {}^2\text{H} \rightarrow {}^4\text{He} + {}^1\text{H} + 18.35$ MeV, and the energy spectrum of the ^{4}He particles produced in the reaction yields the concentration profiles (inset in Fig. 2) directly.

The relation of concentration profiles to the underlying molecular mechanisms is provided through the mutual diffusion coefficient of the two species. The profiles are calculated from Fick's diffusion equation (*16*)

$$\frac{\partial\phi(x)}{\partial t} = \frac{\partial}{\partial x}\left[D(\phi)\frac{\partial\phi(x)}{\partial x}\right] \qquad (2)$$

Here the local concentration ϕ of diffusing species at a distance x from the interface varies with time t in accordance with a mutual diffusion coefficient D that may be strongly dependent on ϕ itself. $D(\phi)$ is the quantity explicitly calculated from the models, and its experimental variation is a measure of the molecular theories. How closely a model approaches reality may also be gauged by how well the experimental interdiffusion profiles are described by Eq. 2 with the appropriate $D(\phi)$, as shown for the profile inset in Fig. 2.

Mixing of Chains with Different Mobilities

Interdiffusion between metals of different atomic mobilities was observed by Kirkendall many years ago (*26*): an excess of the faster atoms diffused into the region of less mobile atoms, creating hydrostatic pressure that led to a bulk or convective flow (flux of vacant lattice sites); this in turn moved a layer of marker atoms separating the two species. For interdiffusing polymers, however, one expects some basic differences, and this has led to controversy concerning the mutual diffusion process. In contrast to metal atoms, polymer chains are entangled with each other, and they translate not by random hops on a lattice but rather by reptation; it is difficult to visualize how convective flow of the slower chains could result from their reptative interpenetration by the more mobile ones. As the compressibility of polymeric liquids is very low, one might expect that, in order for the rapidly diffusing chains to reptate into the region occupied by the slower ones, the latter need first to reptate away to create available space (*27*); otherwise, unacceptable density gradients may be created in the material. Mutual diffusion between polymers would then be dominated by the less mobile species, in contrast to the result expected from the Kirkendall effect.

Experimental studies, carried out by Kramer and co-workers at Cornell, showed the opposite to be true (*23*). Interdiffusion between two polystyrene samples of identical chemical microstructure but with widely differing N values (and hence diffusivities) revealed that a layer of gold marker atoms separating the two polymers moved—evidence of convective flow—at a rate that was controlled by the more mobile chains (*23*). This observation was interpreted in terms of vacancy fluxes or convective flow (*23, 28*), similar to the vacancy fluxes adduced for the metallic interdiffusion effect. There is difficulty in transferring these concepts to entangled polymers, and the interpretation of the polystyrene-marker experiments was criticized on the grounds noted earlier (*29*). The movement of the marker layer, which in these experiments was on the order of a few thousand angstroms at most, was explained as a transient swelling effect reflecting the initial rapid diffusion of the shorter chains during the long relaxation time of the more sluggish ones (*29*). According to this view, over larger spatial scales the mutual diffusion would still be dominated by the slower moving chains. But recent studies (*30, 31*) have shown that, even over macroscopic distances (*31*), as in Fig. 3, interdiffusion between polymers of very widely differing

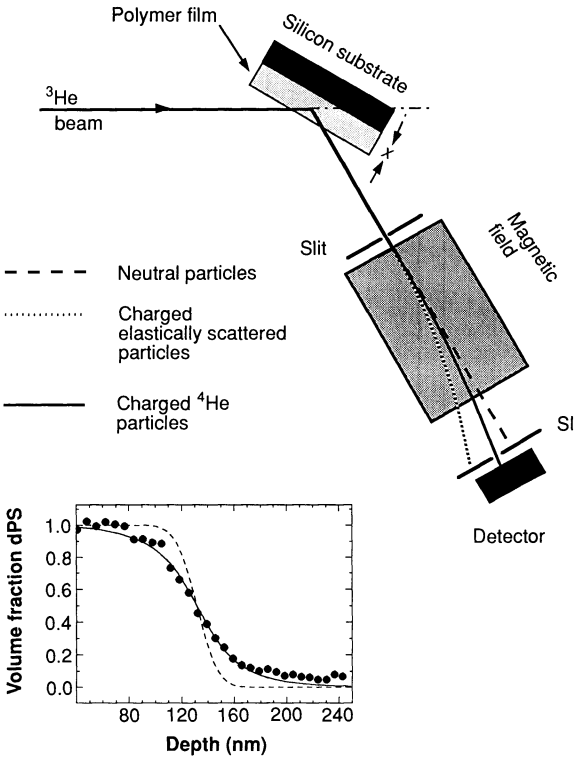

Fig. 2. Schematic illustration of the nuclear reaction analysis experiment (*24*). The ^{3}He beam incident on the polymer bilayer undergoes the reaction

$$^3\text{He} + {}^2\text{H} \rightarrow {}^4\text{He} + {}^1\text{H} + 18.35 \text{ MeV}$$

at depth x, and the magnetic filter allows only ^{4}He particles to reach the detector. The energy of these particles decreases with depth x, and their energy spectrum can be converted into a concentration-depth profile of ^{2}H-labeled chains. This is shown in the inset, which gives the profile at a deuterated polystyrene–protonated polystyrene interface before annealing (broken line) and after 2 hours at 160°C (data points). The solid curve is calculated from the diffusion equation (Eq. 2), making use of the independently determined $D(\phi)$. [Adapted from (*24*) with permission of the American Institute of Physics] diffusivities is controlled by the diffusion coefficient of the more mobile chains. This results in asymmetric concentration profiles, in which the faster moving chains penetrate deeply into the region of the slower ones (Fig. 3).

The weight of experimental evidence today supports the original Cornell observation (*23*): that mutual diffusion between two entangled polymers with different diffusivities is indeed largely controlled by the diffusivity of the more mobile chains. In a molecular picture, which reconciles the different points of view (*23, 28, 32*), the faster diffusing polymers reptate into the region of the more sluggish chains: they do so within an entangling environment, "tubes" due to constraints imposed by the slower molecules, which is itself moving in the opposite direction by a convective (nondiffusive) mechanism, providing the net bulk flow.

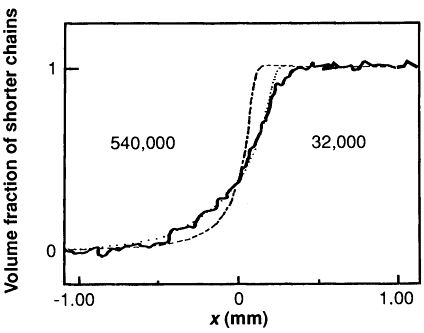

Fig. 3. Concentration profile (determined by infrared microdensitometry) after interdiffusion between short (molecular weight M = 32,000) and long (M = 540,000) polyethylene chains. The dashed and the dotted lines are calculated from models on the assumption that the mutual diffusion is controlled by the slow (longer) or fast (shorter) chains, respectively: the data clearly fit the latter model. [Adapted from (*31*) with permission of the American Chemical Society]

Thermodynamic Slowdown and Acceleration

Polymers that are chemically different may nonetheless fully mix at the molecular level if they are sufficiently compatible, and this despite the very low combinatorial entropy gain driving the mixing. Quantitatively, this happens whenever unfavorable monomeric interactions, as measured by the interaction parameter χ, fall below some critical value χ_c, which is of order $1/N$ (N being the number of monomers on the shorter chains) (*4, 5*). The interaction parameter χ is temperature-dependent, and, for the usual case where dispersive interactions are dominant, decreases with increasing temperature T; this leads to phase equilibrium diagrams with upper critical solution temperatures (inset to Fig. 4). For most polymer pairs, the critical temperature T_c (the temperature at which $\chi = \chi_c$) exceeds their thermal decomposition point, but there are notable exceptions. These occur where the monomers are chemically similar, as in the case of isotopically different but otherwise identical polymers (*33*), or in uncommon (but important) cases where specific, nondispersive interactions between different monomers result in attraction between them, so that χ is negative (*34*). In the former case, where the polymers are fully miscible above T_c, the driving force for mixing may be significantly reduced by the monomeric repulsions (*35*). This leads to thermodynamic slowing down of the interdiffusion between the two species.

The most direct evidence for this slowing down comes from the study by Green and Doyle at Sandia National Laboratories, where the interdiffusion between regular polystyrene (pPS) and its deuterated analog (dPS) was studied as a function of the composition of mixtures of the two (*36*). The results (Fig. 4) show a clear minimum in the interdiffusion rate $D(\phi)$ due to the thermodynamic slowing down. The position of the minimum, at about equal volume fractions of each of the two components, reflects the effect of the repulsive monomer-monomer interactions, which is proportional to $\chi\phi(1 - \phi)$ and is maximal for the symmetric case ($\phi = 0.5$). The detailed variation of $D(\phi)$ with composition ϕ can be calculated from a model that combines the intrinsic diffusivities of the chains with the free-energy changes driving the mixing (*23, 27, 28, 35*). The predicted variation, calculated from the appropriate value of χ, fits the observations closely (Fig. 4). This variation can also be used, via the diffusion equation (Eq. 2), to generate the concentration profiles about the interface between pure dPS diffusing into pure pPS. Such a calculated profile appears as the solid curve in Fig. 2, which well describes the compositional variation across the interface as the two pure polymers interdiffuse.

In contrast to the slowing down described above, which derives from the monomeric repulsions, interdiffusion between two polymers that have a negative χ undergoes what might be termed thermodynamic "acceleration." In this case, mixing is promoted both by the weak entropy of mixing and by the net attractive interactions between the different monomers. This latter effect is locally proportional to $\chi\phi(1 - \phi)$, and, for values of $|\chi|$ that are much larger than $1/N$, can accelerate the interdiffusion process greatly relative to either of the self-diffusion coefficients (*35*). A clear example of this is exhibited by the compatible polymer pair poly(vinyl chloride)/poly(ϵ-caprolactone) (PVC/PCL); for this pair, $\chi = -0.38$, reflecting an attraction between the PVC and PCL monomers thought to arise from a weak dipole-dipole type interaction. For such a large negative χ value, the driving force for interdiffusion is almost entirely due to the mutual monomeric attractions, which vary locally as $\chi\phi(1 - \phi)$, and swamps the contribution (proportional to $1/N$) due to the combinatorial entropy. The mutual diffusion coefficient for this system (shown in Fig. 5A) has a strong maximum around the symmetric ($\phi = 0.5$) composition which maximizes $\phi(1 - \phi)$.

The apparent acceleration of mutual diffusion is magnified for these two polymers by the large disparity in their monomeric friction. A common, if indirect, measure of this disparity is provided by the glass-to-melt transition temperature. This is the temperature below which long-range motion in a melt is frozen out as a result of frictional effects (*37*): a high glass transition temperature implies

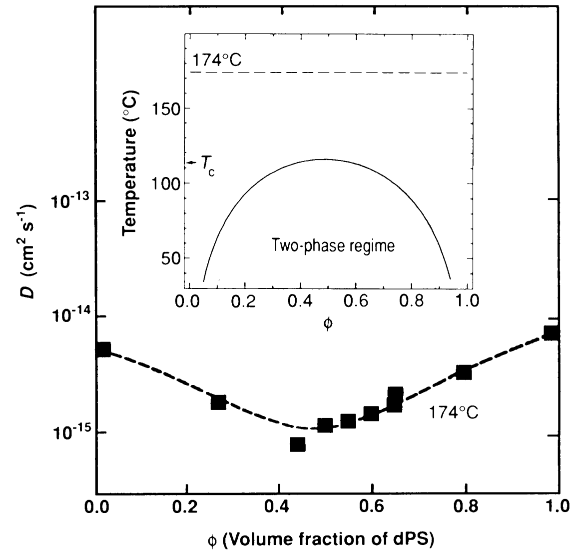

Fig. 4. Variation of the mutual diffusion coefficient $D(\phi)$ for interdiffusion between deuterated polystyrene (dPS) and protonated polystyrene (pPS), as a function of the dPS volume fraction [determined by Green and Doyle using elastic recoil scattering (*36*)]. The diffusion takes place some 60°C above the critical temperature (inset) and clearly shows thermodynamic slowing down, most markedly around $\phi = 0.5$. The dashed line is calculated making use of the appropriate χ parameter for the dPS/pPS system. [Adapted from (*36*) with permission of the American Chemical Society]

large friction between the molecules. As the local composition varies from pure PVC ($\phi = 1$) to pure PCL ($1 - \phi = 1$) across the interface, the glass transition temperature of the blend decreases rapidly and monotonically, with a corresponding increase in local mobility of the interdiffusing chains (*38*). The relation between the blend composition, its glass transition temperature, and the local friction on the diffusing chains, even at temperatures well above the glass transition, is not well understood at a microscopic level; phenomenologically, the large, monotonic increase in chain mobility due to decreasing friction across the interface magnifies the apparent thermodynamic acceleration effect. It results in a maximum in $D(\phi)$ considerably more marked even than the quadratic $\phi(1 - \phi)$ relation (broken curve in Fig. 5A). Other studies of the interdiffusion between polymers with negative χ values, where effects due to differences in the glass transition temperature were minimized (*39*), show a clear enhancement of the mutual diffusivity $D(\phi)$, which is in good agreement with models in which only the thermodynamic driving forces play a role.

For interdiffusion driven primarily by the monomeric attractions, as for PVC/PCL and other systems with negative χ, the overall driving force per polymer chain is directly proportional to N. The topological constraints acting on entangled chains, on the other hand, which force it to reptate, reduce its diffusivity as $1/N^2$ (Eq. 1). Overall, therefore, one expects, and there is some evidence for this (*18*), that the combination of these two effects leads to a mutual diffusivity varying as $[N \times (1/N^2)] = 1/N$ (rather than the inverse square reptation law). For the case of interdiffusion between polymers that are so short that topological effects do not constrain their motion to reptation ("unentangled" chains), an unusual effect is predicted. The driving force for mixing remains proportional to N for the case of large negative χ, but the intrinsic diffusivity in this case no longer obeys the $1/N^2$ reptation law; it varies rather as $1/N$. The net result (for this less common situation of unentangled chains) is a mutual diffusivity independent of the length of interdiffusing chains (*40*).

Finally, the composition dependence of $D(\phi)$ for thermodynamically accelerated interdiffusion can lead to unusual composition profiles about the interface. The solution to the diffusion equation (Eq. 2) with a constant D, for an initially sharp interface between the diffusing species, leads to the classical error function, or Fick's law, profile, with a maximum gradient at the profile midpoint (*16*). For the case in which diffusion is driven primarily by monomeric attractions (χ large and negative), the predicted profile (*27*) is that of a linear composition variation between the interdiffusing species. However, where D exhibits an even stronger maximum about $\phi = 0.5$, arising, for example, from frictional variation as in the PVC/PCL couple, the result is an "anti-Fickian" profile whose composition gradient is a minimum at the profile midpoint. This is seen clearly for interdiffusion between pure PVC and pure PCL (Fig. 5, B and C).

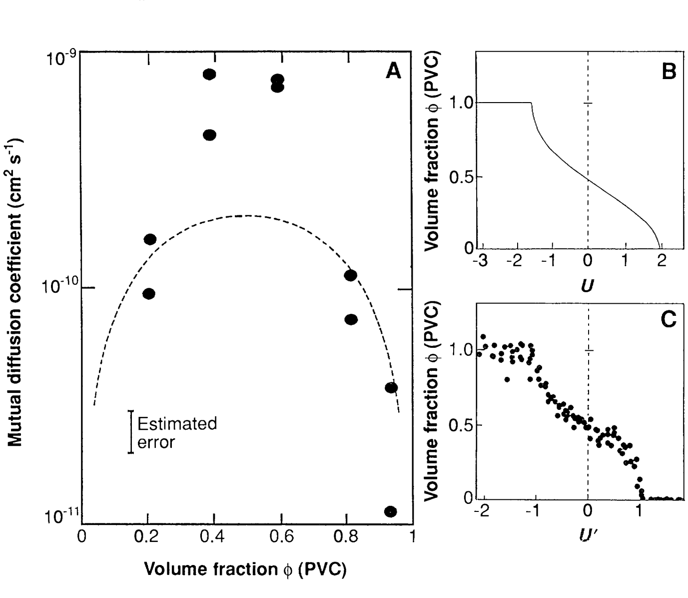

Fig. 5. (**A**) Variation of the mutual diffusion coefficient with the PVC volume fraction ϕ in the compatible pair PVC/PCL at 91°C, determined by microanalytical electron microscopy. The dashed line is the quadratic variation $D_0\phi(1 - \phi)$ (arbitrary D_0) expected for interdiffusing polymers of equal lengths and diffusivities (*19*). The estimated error is based on the scatter in $D(\phi)$ as evaluated from the original interdiffusion profiles (*19, 40*). [Adapted from (*19*) with permission of Macmillan Magazines, Ltd.] (**B**) Concentration profile between interdiffusing PVC and PCL at 91°C calculated from the diffusion equation (Eq. 2) with a $D(\phi)$ taking the PVC and PCL lengths and mobilities into account, which fits the data in (A) more closely than the quadratic variation. U is in units of reduced length $\alpha x t^{-1/2}$, where x is in centimeters, t is in seconds, and $\alpha = 5.10^4$ cm^{-1} s$^{1/2}$ (*38*). (**C**) Interdiffused concentration profile of an initially sharp interface between PVC and PCL at 78°C for the same samples as in (A). U' has the same units as in (B) (direct comparison of scales is inappropriate because of the different temperatures) (*49*).

Interdiffusion Between Partially Miscible Polymers

In the limit of thermodynamic slowing down, the mutual diffusion coefficient in a binary polymer mixture (as in all binary mixtures) goes to zero (*2, 35, 41, 42*). This occurs at the critical point of the phase composition diagram, or more generally between two coexisting phases at temperatures below T_c. Under these conditions, the entropic driving force for mixing is exactly balanced by the repulsive monomeric interactions, resulting in zero net interdiffusive transport. This is the situation for most polymer pairs, which at accessible temperatures are only very partially miscible (*13*). The mobility of the chains, however, remains finite; and two polymeric species in contact at $T < T_c$ will interdiffuse until equilibrium between two coexisting phases, separated by an interfacial mixing zone of finite limiting width w_∞, is established. This interfacial spread is due to the high entropy cost in maintaining too sharp an interface between the two phases (*43*). Interdiffusion in these conditions is then quite different from that in the situations described so far ($T > T_c$), where diffusive mixing between two polymers proceeds without limit and results, in time, in a single homogeneous phase. The width of the mixing zone itself (for $\chi > \chi_c$, that is, $T < T_c$) is predicted (*43, 44*) to vary as $w_\infty = [a/(\chi - \chi_c)^{1/2}]$, where a is comparable with a monomer size. (The divergence of w_∞ at the critical temperature, where $\chi = \chi_c$, corresponds to the onset of unlimited interdiffusion.)

The essential point here is the very small value (around $1/N$) of the critical interaction parameter χ_c, which results from the size of the polymer chains. This result implies that, on the one hand, for highly incompatible polymers (χ on order unity), w_∞ is only a few monomers wide (*45*), as for pairs of incompatible simple liquids. At the same time, there is a large range of χ ($1 >> \chi \gtrsim \chi_c$), and hence temperatures, in which the mixing zone w_∞ becomes sufficiently large, of the order of a polymer coil diameter $a\sqrt{N}$, to permit one to investigate interdiffusion in detail conveniently even in the two-phase regime.

This is seen clearly in Fig. 6, which shows the interdiffusion between the isotopic pair dPS/pPS, which was recently measured in our laboratory both above and below the critical temperature (*44*). In these experiments, nuclear reaction analysis (Fig. 2) was used to determine the concentration profiles across an initially sharp interface between the two polymers. These give the variation with time t of the width w of the interfacial mixing zone, shown in Fig. 6: for temperatures above T_c, the interdiffusion results in an interfacial width w that increases according to the classical $w \propto \sqrt{t}$ law. However, for $T < T_c$, as for the two lower curves in Fig. 6, the interfacial profile develops with time in a very different fashion. After an initial increase, the width w of the mixing zone attains a value indicated by the plateau at long times. This is the limiting interfacial width w_∞; measurements at different temperatures $T < T_c$ (two are shown in Fig. 6) show that w_∞ increases as T_c is approached, and that it agrees quantitatively with the predicted variation, where the temperature-dependent $\chi(T)$ is independently known (*33*).

In addition to broadening an initially sharp interface to its limiting width w_∞, interdiffusion between pure polymeric species below T_c leads also to net transport of chains across the interface until the phases on either side attain their coexistence compositions. For the case where the initial compositions of the polymer phases in contact are already at their coexistence values, however, the interdiffusion is strictly limited to the mixing zone; this situation has been studied (*46*) for isotopic blends (dPS/pPS) at several temperatures in the two-phase regime ($T < T_c$). The initial growth of w (before it reaches its plateau value w_∞) in this case can be described by an apparent power law $w \propto t^\alpha$; the exponent $\alpha = 0.34 \pm 0.06$ is significantly lower than the $\sqrt{t}$ exponent for free interdiffusion. Although this is not yet fully understood (*47*), it underlines the different effects that control the initial interdiffusion rate when the species are not fully miscible.

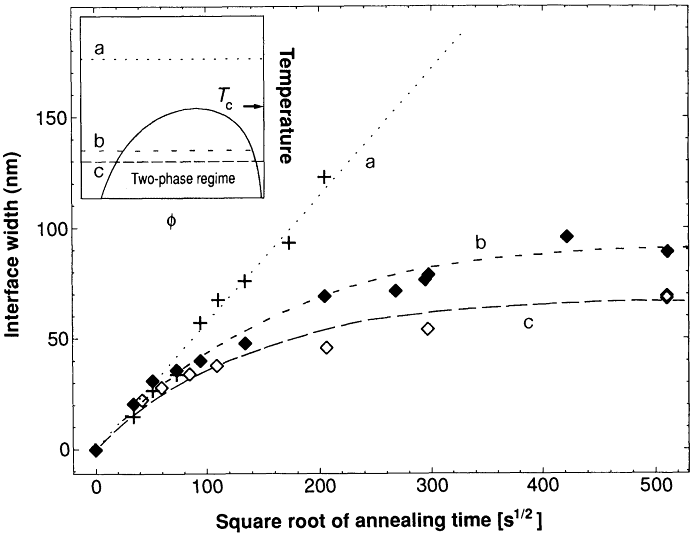

Fig. 6. Interdiffusion broadening of an initially sharp interface between dPS and pPS. Curve a (+) is for a dPS/pPS couple for which the interdiffusion takes place at $T > T_c$ (see schematic inset), showing the interface to broaden as $t^{1/2}$; curves b and c (◆ and ◇, respectively) are for a dPS/pPS couple at two temperatures $T < T_c$ (inset), for which the interfacial width saturates at long times. [Adapted from (*44*) with permission of the American Institute of Physics]

Summary and Prospects

Interdiffusion of high polymers is dominated by a number of factors arising from their long, flexible, chain-like nature. Entanglements strongly suppress (by a factor $1/N^2$) the overall mobility of the chains by constraining them to reptate; their large size greatly diminishes the role of entropy in driving the interdiffusion, on the one hand, and magnifies molecular length scales (by a factor $N^{1/2}$ relative to monomeric liquids), on the other; and intrinsic monomeric friction can vary greatly between interdiffusing species, in a way that is enhanced relative to the case for simple liquids by the need for cooperative motion of monomers on a given chain. Taken together, these factors are responsible for the extreme variability of both the spatial and the temporal scales of diffusional processes in polymers. Changes in these scales of many orders of magnitude are provided through changes in N, and through minor changes in the monomer chemistry and in the temperature, an effect not conceivable for simple liquids. The long times and large dimensions associated with molecular diffusion processes in polymeric liquids make possible convenient and direct experimentation and thus the probing of more general phenomena in the liquid state, especially near critical points.

Future work can proceed along several avenues. These relate both to basic concepts and to phenomena, outlined earlier, deriving from the interdiffusion process. The cooperative friction effects noted above result in glass transition temperatures (*37*) for polymers that are generally very much higher than those for the corresponding monomer liquids. In addition, these effects lead to enhanced friction also at temperatures that are well above this glass-to-melt transition. These temperature-dependent friction effects have long been recognized and can be accounted for empirically (*3*) but are not as well understood at the molecular level as the entanglement or thermodynamic factors. Studies of mutual diffusion between different polymers with controlled microstructure (for example, the size of side groups on monomers, or monomer polarizability) and blend composition, as well as studies of their self-diffusion, will lead to a better microscopic insight into this frictional aspect of interdiffusive transport.

Refinements to the original reptation model, investigated over the last decade in polymeric self- and tracer-diffusion studies (*8, 9*), such as the transport of nonlinear chains, and relaxations arising from the nonrigidity of "tubes" in a melt (*12*), can be extended also to interdiffusion between chemically different chains. "Tube" relaxation, in particular, may be more marked in a mixture where the different monomer microstructures result in large differences in chain mobilities. Diffusional processes involving diblock copolymers with chemically disparate blocks, which can self-assemble in the bulk or segregate at interfaces, with clear analogies in systems of flexible biological macromolecules (*48*), are a particular example for which there is considerable practical interest.

An important aspect of polymer interdiffusion that has not been investigated in detail to date has to do with the configuration of chains near surfaces or interfaces, or more generally in confined geometries, and in particular the disposition of chain ends, which must differ from that in the unrestricted bulk. As reptation proceeds exclusively through such ends, interdiffusion between two polymers whose surfaces are placed in contact to form a sharp interface, for example, must initially depend on the rate at which the chain ends can access this interface. This question is intimately related to the welding and adhesion of polymeric materials, and to diffusional processes associated with polymers in thin films or small pores (especially for dimensions comparable with a coil size). Only recently have experimental methods such as x-ray and neutron reflectometry, which can determine structure at the scales necessary for studying this effect at a single planar interface, been applied to polymers. In combination with more direct profiling methods, such techniques can probe interdiffusion and structure in the first few nanometers about the interface and shed light on the perturbing effect of the interface itself on adjacent chains.

REFERENCES AND NOTES

1. J. S. Rowlinson, *Liquids and Liquid Mixtures* (Butterworth, London, ed. 2, 1969).
2. R. B. Bird *et al.*, *Transport Phenomena* (Wiley, New York, 1960).

3. J. D. Ferry, *Viscoelastic Properties of Polymers* (Wiley, New York, ed. 3, 1980); W. W. Graessley, in *Molecular Conformation and Dynamics of Macromolecules in Condensed Systems*, M. Nagasawa, Ed. (Elsevier, Amsterdam, 1988), p. 163.
4. P. J. Flory, *Principles of Polymer Chemistry* (Cornell Univ. Press, Ithaca, NY, 1953).
5. P. G. de Gennes, *Scaling Concepts in Polymer Physics* (Cornell Univ. Press, Ithaca, NY, 1979).
6. S. F. Edwards, *Proc. Phys. Soc. (London)* **92**, 9 (1967); *Polymer* **9**, 140 (1977).
7. P. G. de Gennes, *J. Chem. Phys.* **55**, 572 (1971).
8. J. Klein, *Nature* **271**, 143 (1978).
9. ———, *Contemp. Phys.* **20**, 611 (1979); W. W. Graessley, *Adv. Polym. Sci.* **47**, 67 (1982); M. Tirrell, *Rubber Chem. Technol.* **57**, 523 (1984); J. Klein, in *Encyclopedia of Polymer Science and Engineering* (Wiley, New York, ed. 2, 1987), p. 205; D. Pearson, *Rubber Chem Technol.* **60**, 439 (1987); F. Brochard-Wyart, in *Fundamentals of Adhesion*, T. D. Lee, Ed. (Plenum, New York, 1988), p. 243; K. Binder and H. Sillescu, in *Encyclopedia of Polymer Science and Engineering* (Wiley, New York, ed. 2, 1989), p. 297; H. H. Kausch and M. Tirrell, *Annu Rev. Mater. Sci.* **19**, 341 (1989).
10. M. Doi and S. F. Edwards, *The Theory of Polymer Dynamics* (Oxford Univ. Press, Oxford, 1986).
11. L. S. Lerman and H. L. Frisch, *Biopolymers* **21**, 995 (1982); P. G. de Gennes, *C. R. Acad. Sci. Ser. II* **294**, 827 (1982); see also O. J. Lumpkin and B. H. Zimm, *Biopolymers* **21**, 2315 (1982).
12. J. Klein, *Macromolecules* **11**, 852 (1978); M. Daoud and P. G. de Gennes, *J. Polym. Sci. Polym. Phys.* **17**, 1971 (1979); P. F. Green, P. J. Mills, C. J. Palmstrom, J. W. Mayer, E. J. Kramer, *Phys. Rev. Lett.* **53**, 2145 (1984).
13. D. R. Paul and S. Newman, Eds., *Polymer Blends* (Academic Press, New York, 1978); O. Olabisi, L. M. Robeson, M. T. Shaw, Eds., *Polymer-Polymer Miscibility* (Academic Press, New York, 1979).
14. F. Bueche, W. M. Cashin, P. Debye, *J. Chem. Phys.* **20**, 1956 (1952).
15. M. Doi and S. F. Edwards, *J. Chem. Soc. Faraday Trans. II* **74**, 1789 (1978); *ibid.*, p. 1802; *ibid.*, p. 1818.
16. J. Crank, *Mathematics of Diffusion* (Oxford Univ. Press, Oxford, ed. 2, 1975).
17. J. Klein and B. J. Briscoe, *Proc. R. Soc. London Ser. A* **365**, 53 (1979).
18. F. P. Price, P. T. Gillmore, E. L. Thomas, R. L. Laurence, *J. Polym. Sci. Polym Symp.* **63**, 33 (1978); *Macromolecules* **13**, 880 (1980). [See also A. Y. Chalykli *et al*, *Polym. Sci. U.S.S.R.* **21**, 1835 (1980); *ibid.*, p. 2579.]
19. R. A. L. Jones, J. Klein, A. M. Donald, *Nature* **321**, 161 (1986).
20. G. Coulon *et al.*, *Macromolecules* **22**, 2581 (1989).
21. T. P. Russel, A. Karim, A. Mansour, G. P. Felcher, *ibid.* **21**, 1890 (1988); M. L. Fernandez *et al.*, *Polymer* **29**, 1923 (1988).
22. G. Reiter, S. Hüttenbach, M. Foster, M. Stamm, *Macromolecules*, in press.
23. E. J. Kramer, P. F. Green, C. J. Palmstrom, *Polymer* **25**, 473 (1984).
24. U. K. Chaturvedi *et al.*, *Appl. Phys. Lett.* **56**, 1228 (1990).
25. P. J. Mills *et al.*, *ibid.* **45**, 957 (1984); J. Sokolov *et al.*, *ibid* **54**, 590 (1989).
26. E. D. Kirkendall, *Trans Am. Inst. Min. Metall Eng.* **147**, 104 (1942); L. S. Darken, *ibid.* **175**, 184 (1948).
27. F. Brochard-Wyart, J. Jouffray, P. Levinson, *Macromolecules* **16**, 1638 (1983).
28. H. Sillescu, *Makromol. Chem. Rapid Commun.* **5**, 519 (1984).
29. F. Brochard-Wyart and P. G. de Gennes, *Europhys. Lett.* **1**, 221 (1986).
30. R. J. Composto, E. J. Kramer, D. M. White, *Nature* **328**, 234 (1987).
31. E. A. Jordan *et al.*, *Macromolecules* **21**, 235 (1988).
32. F. Brochard-Wyart, in *Molecular Conformation and Dynamics of Macromolecules in Condensed Systems*, M. Nagasawa, Ed. (Elsevier, Amsterdam, 1988), p. 249.
33. A. D. Buckingham and H. G. Hentschel, *J. Polym Sci. Polym Phys.* **18**, 853 (1980); F. S. Bates, G. D. Wignall, W. C. Koehler, *Phys Rev. Lett.* **55**, 2425 (1985); *ibid.* **57**, 1429 (1986).
34. For such polymer pairs ($\chi < 0$), the phase diagram is frequently characterized by a lower critical solution temperature (*13*), although in this review I make reference only to the usual case of an upper critical temperature.
35. P. G. de Gennes, *J Chem. Phys.* **72**, 4756 (1980).
36. P. F. Green and B. L. Doyle, *Phys. Rev. Lett.* **57**, 2407 (1986); *Macromolecules* **20**, 2471 (1987).
37. G. Gee, *Contemp. Phys.* **11**, 313 (1970).
38. R. A. L. Jones, thesis, Cambridge University, Cambridge (1987).
39. R. J. Composto *et al*, *Phys. Rev Lett.* **57**, 1312 (1986).
40. J. Kanetakis and G. Fytas, *J. Chem. Phys.* **87**, 5048 (1987).
41. P. Pincus, *ibid.* **75**, 1996 (1981); K. Binder, *ibid.* **79**, 6387 (1983).
42. A homogeneous polymer mixture taken from the one-phase to the two-phase region will demix spontaneously (spinodally) into coexisting phases (*4, 5, 41*); this type of diffusive process is related to the present section but will not be considered separately.
43. E. Helfand and A. M. Sapse, *J Chem. Phys.* **62**, 1327 (1975); L. Leibler, *Macromolecules* **15**, 1283 (1982).
44. U. K. Chaturvedi *et al.*, *Phys. Rev. Lett.* **63**, 616 (1989).
45. T. Hashimoto, M. Shibayama, H. Kawai, *Macromolecules* **13**, 1237 (1980).
46. U. Steiner, G. Krausch, G. Schatz, J. Klein, *Phys Rev. Lett.* **64**, 1119 (1990).
47. P. G. de Gennes, *C. R. Acad. Sci. Ser. II* **308**, 13 (1989); J. L. Harden, *J. Phys France* **51**, 1777 (1990).
48. R. Gelman, D. C. Poppke, K. A. Piez, *J. Biol. Chem.* **255**, 8098 (1980).
49. R. A. L. Jones *et al*, in preparation; S. Rocca and J. Klein, unpublished data.
50. I thank Z. Alexandrowicz, E. Katzir, Y. Rabin, S. Reich, G. Schatz, A. Silberberg, and U. Steiner for useful comments on the manuscript, and M. Eisenstein and U. Steiner for help with the figures. This work was supported by the German-Israel Foundation, the U.S.–Israel Binational Science Foundation, and the Minerva Foundation. The author is the Herman Mark Professor of Polymer Physics at the Weizmann Institute.

Research Articles

A Thermodynamic Scale for the Helix-Forming Tendencies of the Commonly Occurring Amino Acids

KARYN T. O'NEIL AND WILLIAM F. DEGRADO

Amino acids have distinct conformational preferences that influence the stabilities of protein secondary and tertiary structures. The relative thermodynamic stabilities of each of the 20 commonly occurring amino acids in the α-helical versus random coil states have been determined through the design of a peptide that forms a noncovalent α-helical dimer, which is in equilibrium with a randomly coiled monomeric state. The α helices in the dimer contain a single solvent-exposed site that is surrounded by small, neutral amino acid side chains. Each of the commonly occurring amino acids was substituted into this guest site, and the resulting equilibrium constants for the monomer-dimer equilibrium were determined to provide a list of free energy difference (ΔΔG°) values.

HOW AN AMINO ACID SEQUENCE DICTATES THE THREE-dimensional structure of a protein is an intriguing, but largely unsolved question. While a general solution to the protein folding problem is not yet available, considerable progress has been made in understanding the factors stabilizing α helices. Each amino acid has distinct conformational preferences that lead to stabilization or destabilization of an α helix (*1*). Electrostatic interactions between charged side chains and either the helical